SCIENTIFIC REPORTS

OPEN

SUBJECT AREAS:
STABLE ISOTOPES
BIOGEOCHEMISTRY

Received
23 April 2014

Accepted
3 June 2014

Published
23 June 2014

Correspondence and requests for materials should be addressed to S.B. (steven.bouillon@ees.kuleuven.be)

Contrasting biogeochemical characteristics of the Oubangui River and tributaries (Congo River basin)

Steven Bouillon[1], Athanase Yambélé[2], David P. Gillikin[3], Cristian Teodoru[1], François Darchambeau[4], Thibault Lambert[4] & Alberto V. Borges[4]

[1]Department of Earth and Environmental Sciences, KULeuven, Leuven, Belgium, [2]Service de l'Agrométéorologie et de Climatologie, Direction de la Météorologie Nationale, Bangui, Central African Republic, [3]Department of Geology, Union College, Schenectady, NY, USA, [4]University of Liège, Chemical Oceanography Unit, Liège, Belgium.

The Oubangui is a major tributary of the Congo River. We describe the biogeochemistry of contrasting tributaries within its central catchment, with watershed vegetation ranging from wooded savannahs to humid rainforest. Compared to a 2-year monitoring record on the mainstem Oubangui, these tributaries show a wide range of biogeochemical signatures, from highly diluted blackwaters (low turbidity, pH, conductivity, and total alkalinity) in rainforests to those more typical for savannah systems. Spectral analyses of chromophoric dissolved organic matter showed wide temporal variations in the Oubangui compared to spatio-temporal variations in the tributaries, and confirm that different pools of dissolved organic carbon are mobilized during different hydrological stages. $\delta^{13}C$ of dissolved inorganic carbon ranged between −28.1‰ and −5.8‰, and was strongly correlated to both partial pressure of CO_2 and to the estimated contribution of carbonate weathering to total alkalinity, suggesting an important control of the weathering regime on CO_2 fluxes. All tributaries were oversaturated in dissolved greenhouse gases (CH_4, N_2O, CO_2), with highest levels in rivers draining rainforest. The high diversity observed underscores the importance of sampling that covers the variability in subcatchment characteristics, to improve our understanding of biogeochemical cycling in the Congo Basin.

The recognition that carbon (C) processing within inland waters could be a substantial component in C budgets at the catchment, regional, or global scale (e.g.[1–3]), has led to an increased momentum in studies on riverine biogeochemistry. Further constraining the role of river systems will only be possible by generating additional comprehensive datasets, in particular on systems or regions which are currently underrepresented. Of key importance are tropical and subtropical regions, which have been suggested to be of particular importance in terms of riverine transport of sediments and carbon (e.g.[4–5]), and have been suggested to show higher areal CO_2 outgassing rates than their temperate or boreal counterparts[3,6]. Based on a long tradition of interdisciplinary studies, the Amazon often serves as a model system for the biogeochemical functioning of tropical river basins with African rivers being largely neglected. The Congo River basin is second to the Amazon in terms of discharge (1310 versus 6640 $km^3\ yr^{-1}$) and catchment size (3.8 10^6 versus 5.8 10^6 km^2), but is much less well characterized from a hydrological, physico-chemical, and biogeochemical point of view. The main biogeochemical studies on the Congo basin have focussed on dissolved and particulate erosion rates both on the main Congo River and in some of its major tributaries such as the Oubangui and Sangha (e.g.,[7–11]). The synthesis of Laraque et al.[11], however, shows that sampling efforts were concentrated on a limited number of sites, and these monitoring programmes were limited to a restricted number of basic parameters. For many stations, extrapolations needed to be made based on less than 5 samples (e.g. the upper Congo River and Kasai River[12],). Mariotti et al.[13] provided the first stable isotope data on particulate organic carbon (POC) from the lower Congo River and some of its tributaries. More recently, some explorative work on the organic and inorganic C biogeochemistry of the lower Congo River has been presented[14–46], and we reported results from a 1-year sampling programme on the Oubangui at Bangui (Central African Republic, CAR), focussing on the dynamics and annual export of different C pools and greenhouse gas (GHG) emissions[17]. Rivers in the Congo basin network, however, can be expected to show highly variable physico-chemical and biogeochemical characteristics, considering the range in geology, climatic conditions and land use/vegetation across the basin. Laraque et al.[18] analysed the physico-chemical properties and major ion composition in different tributaries of the lower Congo, and found strong contrasts between those draining the

"Cuvette Congolaise" (mainly rainforest-dominated lowlands) and the "Téké plateaux", where savannahs form the main biome type. Similarly, Mann et al.[19] recently demonstrate strong gradients in biogeochemical characteristics across rivers and streams in the Sangha and lower Oubangui catchment. The existence of a large gradient in biogeochemical characteristics is relatively well documented for some of the large South American basins (e.g.[20]), but comprehensive geochemical data from the Congo basin are still mostly limited to the mainstem in the Malebo Pool at Brazzaville and some of the main tributaries. During three sampling campaigns between 2010 and 2012, we sampled a number of tributaries of the Oubangui River, from savannah-dominated systems (Mbali River, Mpoko River) to those draining mainly humid rainforest ecosystems (Lobaye, Mbaéré, Bodingué, and some of their minor tributaries) in the Ngotto Forest (Figure 1). Here, we compare biogeochemical data from these tributaries with our own results from 2 years of high-frequency sampling on the mainstem Oubangui River at Bangui, and with available literature data on the wider Congo Basin.

Results

Material fluxes in the Oubangui River. A detailed discussion of results for the first year of monitoring was presented in Bouillon et al.[17]. While no direct DOC measurements are available for the 2nd year, we estimated DOC fluxes based on the relationship between a_{350} and DOC observed in the tributaries (see Supplement Figure S1; unpublished data from other sites within the larger Congo Basin also follow this trend). The 2nd year of measurements was characterized by a markedly lower annual discharge (~30% lower), and for most elements, the annual transport fluxes were accordingly lower than those reported previously by 22% (for DIC) to 55% (for DOC, summarized in Table 1). As an illustration, the seasonal patterns over both years of sampling are presented in Figures 2–3 for TSM, TA, $\delta^{13}C_{DIC}$, pCO_2, CH_4 and N_2O. The full data can be found in[17] and in Supplementary Table 2. During the 2nd year, however, we also analysed spectral parameters of cDOM. The a_{350} values exhibited a strong increase with increasing discharge, with values ranging from about 5 m^{-1} during base flow to > 20 m^{-1} during high flow (Figure 4). The a_{250}:a_{365} ratio values were relatively high during base flow (4.6–5.5) and dropped markedly during the ascending limb of the hydrograph to values closed to 4.2 during high flow period (Figure 4). Opposite patterns were observed for the spectral slopes. $S_{275-295}$ values decreased with increasing discharge (from >0.016 nm^{-1} during base flow to 0.012 nm^{-1} during high flow) whereas $S_{350-400}$ values increased with increasing discharge (from 0.013 nm^{-1} during base flow to 0.016 nm^{-1} during high flow). Finally, spectral slope ratios (S_R) exhibited a strong seasonal variation with markedly higher values during base flow period (>1.2) compared to high flow period (about 0.8).

Despite the lower transport fluxes, estimated CO_2 fluxes across the water-air interface were similar or slightly higher during 2011–2012 than during 2010–2011 (Table 1). Overall, the seasonality in concentrations and isotope ratios followed similar patterns during both years (Figures 2–3), hence we will not discuss these in detail but use the data mainly to examine overall patterns across the mainstem and tributaries.

Tributary characteristics. Tributaries showed a much wider range of values for most of the measured variables than recorded during the

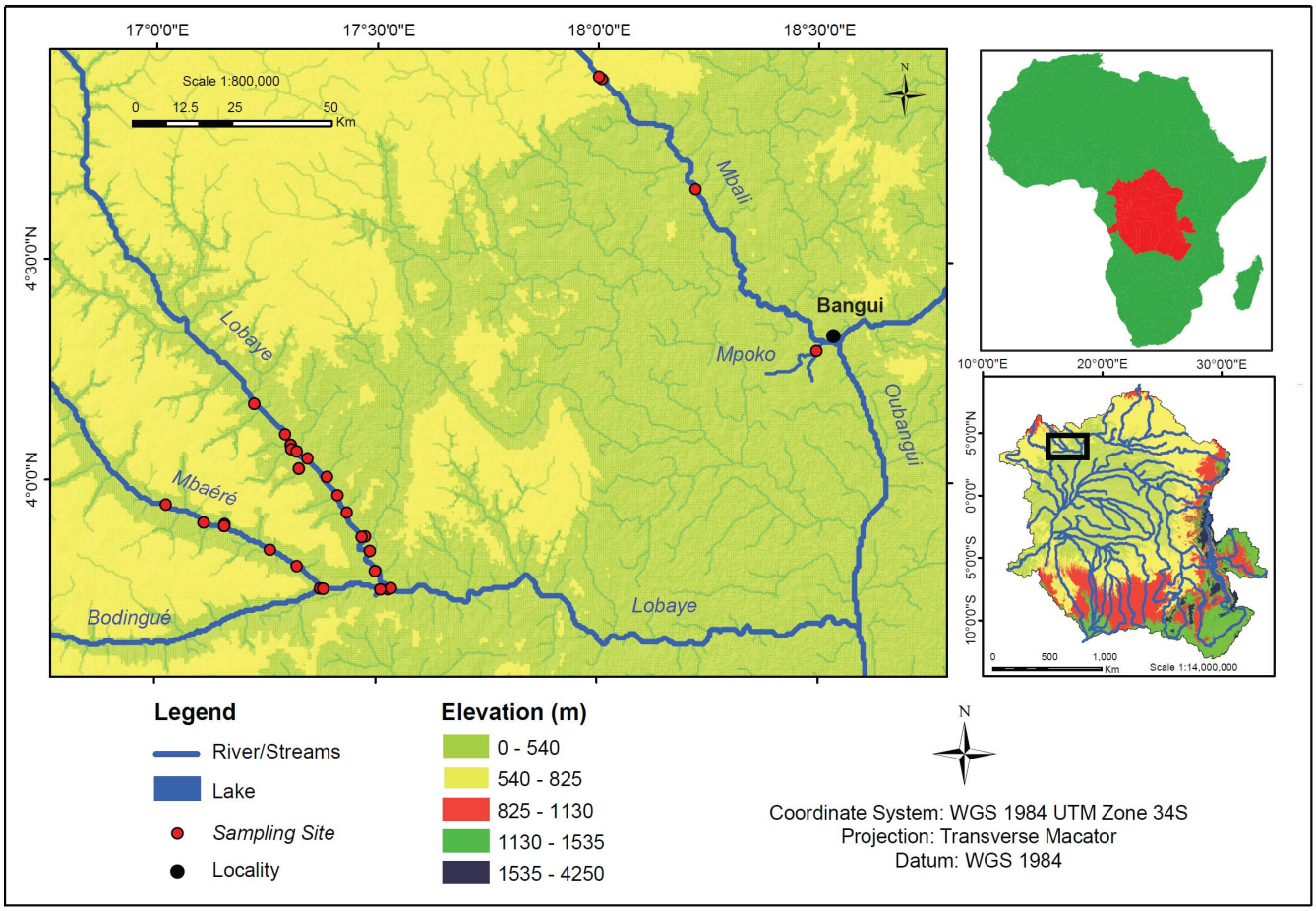

Figure 1 | Map showing the location of the Oubangui within the Congo Basin, and detailed map showing the tributary sampling sites (note that some sites represent small first order tributaries). Map produced using ArcGIS software.

Table 1 | Summary of fluxes and element ratios, and yields (i.e. fluxes expressed per unit are of the catchment) measured in the Oubangui River at Bangui during two subsequent hydrological years, 20th March 2010 to 19th March 2011 (data from Bouillon et al. 2012) and 20th March 2011 to 18th March 2012 (this study). Fluxes are expressed in Tg y^{-1}, yields are expressed in ton km^{-2} y^{-1}

Constituent	Flux, 2010–2011	Flux, 2011–2012	Yield, 2010–2011	Yield, 2011–2012
Discharge (m^3 s^{-1})	3361	2343		
TSM	2.45	1.63	5.01	3.33
POC	0.1446	0.0889	0.296	0.182
PN	0.0142	0.0100	0.029	0.020
DOC	0.725	0.323[a]	1.483	0.661
DIC	0.479	0.374	0.980	0.765
%POC	5.9	5.5		
POC/PN (mass based)	10.2	8.9		
Annual water-air CO_2 flux (mmol CO_2 m^{-2} d^{-1})[1]	24.5[b]–46.7[c]	28.9[b]–53.3[c]		

a: estimated based on relationship between a_{350} and DOC concentrations, see text and Supplementary Figure S1. b, c: calculated using two different parameterisations, see[17] for details.

2 years of monitoring on the mainstem Oubangui River. Biogeochemical signatures in the tributaries appear to be clustered according to the catchment characteristics. Specific conductivity generally showed very low values (average 14.6 µS cm^{-1}, with a minimum of 7.6 µS cm^{-1}) in many sites within the densely vegetated Ngotto Forest (Lobaye, Mbaéré, Bodingué), and was higher in the more northern, savannah catchments (Mbali, Mpoko : 22–170 µS cm^{-1}) as well as in all left bank tributaries of the Lobaye river (average 89.4 µS cm^{-1}) which are situated at the rainforest/savannah transition. TA was generally well correlated with specific conductivity (Figure 5), and ranged between 0.009 and 1.791 mmol L^{-1}. The highly dilute rivers in rainforest-dominated catchments were also characterised by very low TSM concentrations (0.7–16.0 mg L^{-1}) while higher TSM loads were encountered in some of the tributaries of the Lobaye (9.4–44.4 mg L^{-1}) and in Mpoko River (78.0 mg L^{-1}). Rivers in the Ngotto Forest were also characterized by relatively lower pH values, but despite the visual appearance as 'blackwater' rivers (in particular the Mbaéré and Bodingué), do not show substantially higher DOC concentrations (between 1 and 6 mg L^{-1} for the majority of samples, Figure 6). The a_{350} values of the Oubangui tributaries were higher during the wet period (36.2 ± 14.0 m^{-1}) than during the dry period (22.9 ± 6.8 m^{-1}) (see Supplementary Tables) and are well correlated with DOC concentrations across the seasons (Figure S1). The variations of a_{250}:a_{365} ratios were relatively limited within and across seasons, with a pattern of lower values during wet period (3.84 ± 0.16) compared to the dry period (4.02 ± 0.17). Spectral slopes over the range 275–295 nm ($S_{275-295}$) decreased weakly between the dry and wet period, with mean values of 0.0124 ± 0.0004 nm^{-1} and 0.0116 ± 0.0003 nm^{-1}, respectively. In contrast, $S_{350-400}$ values tended to be higher during wet period (0.0152 ± 0.001 nm^{-1}) compared to dry period (0.0147 ± 0.0009 nm^{-1}). The difference in the S_R ratio was however more marked between the two seasons, with lower values during the wet period (0.770 ± 0.049) compared to the dry period (0.845 ± 0.046). Note that the variations of DOM composition proxies were more marked when data are compared site to site. For example, the increase in a_{350} in the Mbaéré from 10.5 to 35.0 m^{-1} between dry and wet periods was related to clear decreases in the a_{250}:a_{365} ratio (from 4.3 to 3.7), $S_{275-295}$ (from 0.0131 to 0.0117 nm^{-1}) and S_R (from 0.860 to 0.799). Compared to the mainstem Oubangui River, $\delta^{13}C$ values of DIC span a wide range of values and are typically more ^{13}C-depleted, with very low values in the Mbaéré (−23.5 ± 2.0‰), intermediate values in the mainstem Lobaye (−16.1 ± 2.0‰) and in its minor tributaries (−14.3 ± 2.3‰), and highest values in the Mbali and Mpoko River (−11.1 to −10.5‰). $\delta^{13}C_{DIC}$ values are strongly negatively correlated with pCO_2 (Figure 7). With the exception of the Mpoko River, $\delta^{13}C$ values of POC and DOC fall within the range expected for a dominance of C3 vegetation (−31.2 to −25.8‰ for POC, −30.6 to −27.0 for DOC). The more turbid Mpoko River showed a $\delta^{13}C_{POC}$ of −22.8‰, indicating a substantial contribution from C4 vegetation in this subcatchment (no $\delta^{13}C_{DOC}$ data available for this site). $\delta^{13}C$ values of POC and DOC pools were well correlated, and $\delta^{13}C_{POC}$ values increased with TSM load (Figure 8).

Calculated pCO_2 values for the different Oubangui tributaries were highly variable, ranging between 870 and 33500 ppm, being generally higher than those observed in the mainstem Oubangui River (Figure 9). Similarly, both dissolved CH_4 and N_2O concentrations were generally higher in tributaries than in the mainstem Oubangui River (Figure 9).

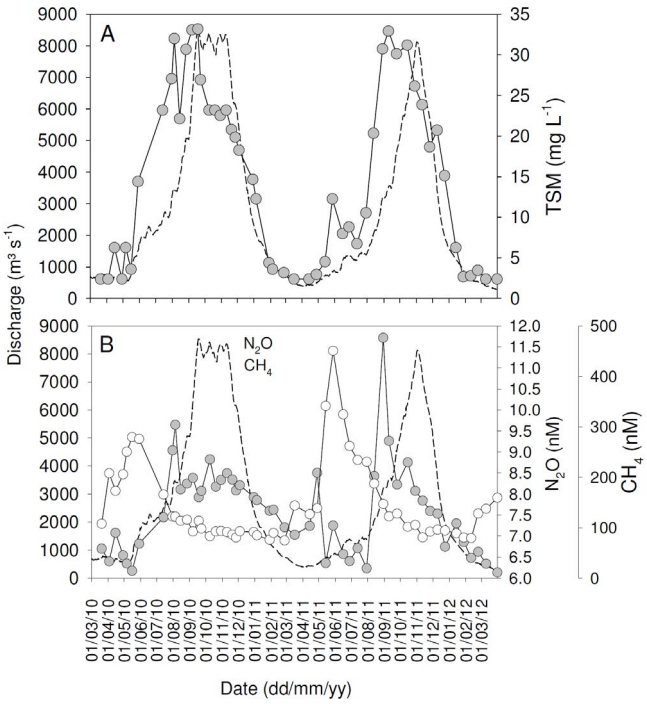

Figure 2 | Seasonal variations of daily discharge (dotted lines) and (A) total suspended matter concentrations (TSM), and (B) concentrations of CH_4 and N_2O in the Oubangui River at Bangui between March 2010 and March 2012.

Discussion

Organic carbon. Rivers are often categorized in one of three types, mainly based on colour, distinguishing white-water rivers (alkaline to neutral pH, high sediment loads), black-water rivers (acidic, high DOC loads, very low sediment loads and dissolved ion concentrations), and clear-water rivers (low sediment loads but

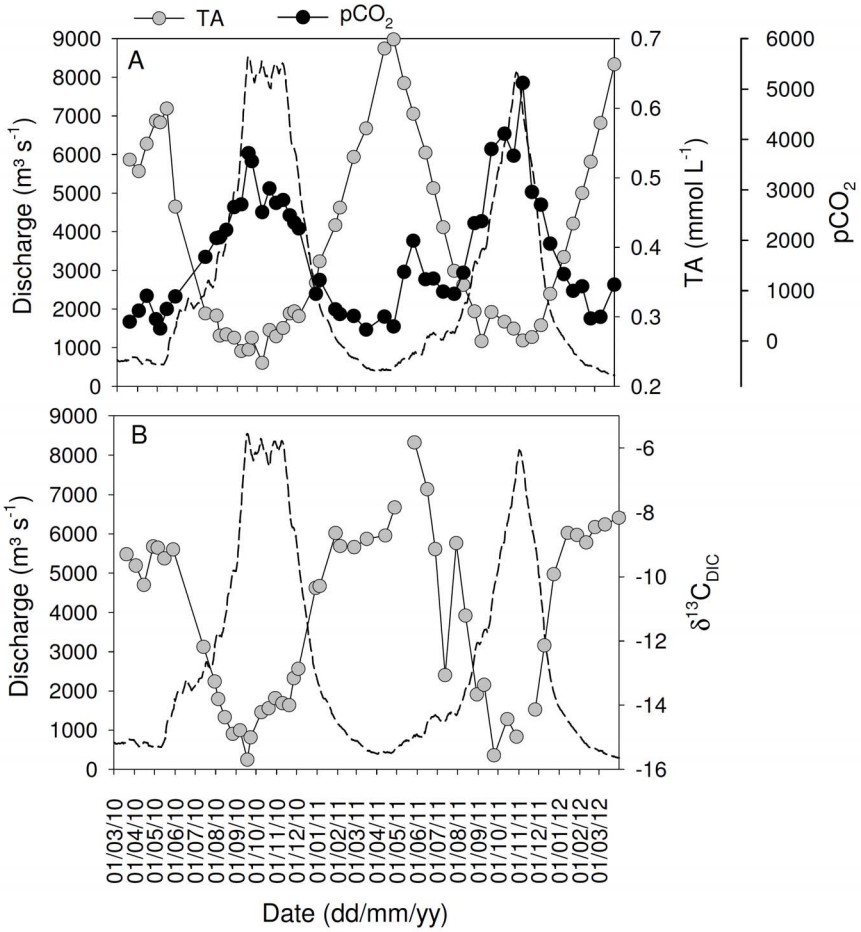

Figure 3 | **Seasonal variations of daily discharge (dotted lines) and (A) total alkalinity (TA) and the partial pressure of CO_2 (pCO_2), and (B) the carbon stable isotope signatures of dissolved inorganic carbon ($\delta^{13}C_{DIC}$) in the Oubangui River at Bangui between March 2010 and March 2012.**

variable in terms of pH and alkalinity). This distinction is, however, not always straightforward (see e.g. 21). Consistent with the generally low mechanical erosion rates reported for the Congo Basin[11], TSM concentrations in most of the tributaries were low. Only the Mpoko River which drains a wooded savannah region and some of the minor tributaries of the Lobaye, on the rainforest-savannah transition zone, showed slightly more elevated TSM concentrations (9.0–78.0 mg L^{-1}). While the Bodingué and Mbaéré watersheds sampled here visually show characteristics of blackwater rivers, their DOC concentrations (1.5–7.1 mg L^{-1}) in the lower range of those found in the mainstem Oubangui (Figure 8), and generally lower than those reported for the mainstem Congo River (6.2 to 17.6 mg L^{-1}; 13,19) or the Epulu River in the upper Congo Basin (5.2–9.0 mg L^{-1}; Spencer et al. 2010), and lower than the range reported for blackwater rivers in the Amazon (7–40 mg L^{-1}, 21). In all of the sampled tributaries, DOC remained the dominant form of organic C (OC), representing 53–95% of the total OC pool. While sampling sites were not consistently similar between different sampling campaigns, DOC concentrations were generally higher during the 2012 wet season compared to the 2 dry season campaigns (e.g. for the mainstem Lobaye: 3.5 ± 0.9 mg L^{-1}, n=5 during the wet season, 1.9 ± 0.1 mg L^{-1}, n=5 during dry season; for the Mbaéré: 6.4 ± 1.0 mg L^{-1}, n=2 during the wet season, 2.4 ± 0.8 mg L^{-1}, n=6 during dry season). Such higher DOC concentrations during wet conditions are in line with results from other sites in the Congo basin such as the mainstem Oubangui[10,17], mainstem Congo[10,16], and rivers in the Ituri Forest[14].

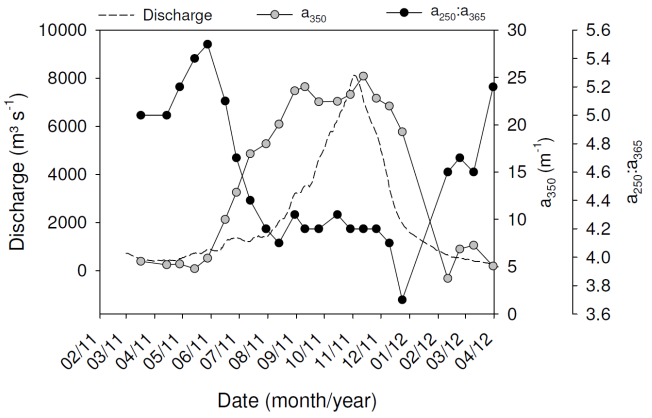

Figure 4 | **Seasonal variations of a_{350} and the a_{250}:a_{365} ratio in the mainstem Oubangui River between March 2011 and April 2012.**

The ratio of spectral slopes S_R and the a_{250}:a_{365} ratio were developed as rapid and easy methods for characterizing cDOM. The S_R ratio has been correlated to molecular weight and sources, i.e samples of greater allochthonous contribution with higher molecular weight DOM have lower S_R values[22]. The a_{250}:a_{365} ratio has been correlated with the molecular size and DOM aromaticity with decreasing values relating to increasing molecular size[23]. In a recent study focusing on cDOM properties in 30 U.S Rivers, Spencer et al.[24] also showed that the a_{250}:a_{365} ratio was inversely related to the hydrophobic organic acid fraction (HPOA) of DOM which represents the high molecular weight, aromatic-dominated fraction of DOM[25]. Therefore, low a_{250}:a_{365} ratio values (high HPOA fraction)

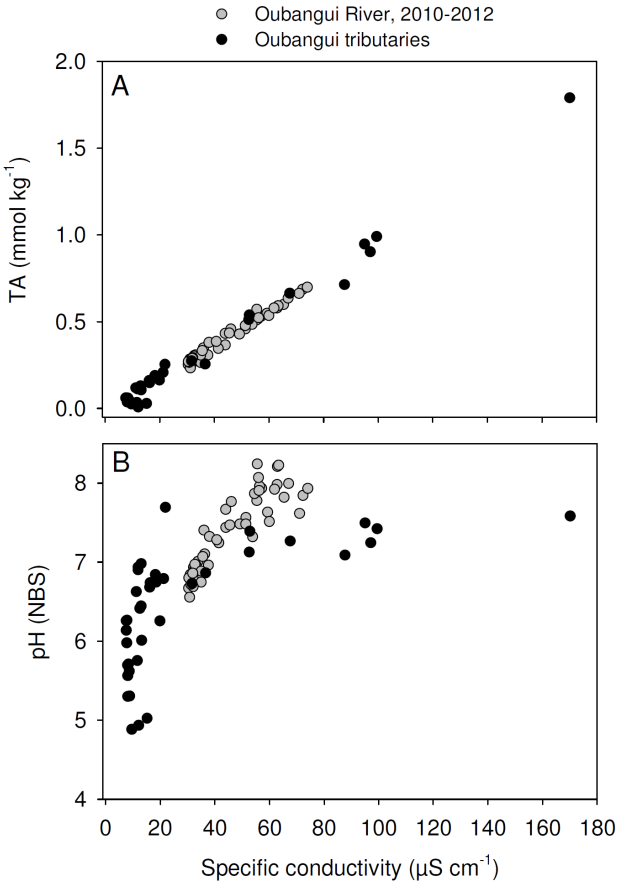

Figure 5 | Relationships between specific conductivity and (A) total alkalinity (TA), and (B) in situ pH for the mainstem Oubangui (grey circles; data from 2 years of monitoring), and tributaries of the Oubangui (black circles).

indicate an allochthonous origin of DOM, whereas high a_{250}:a_{365} values (low HPOA fraction) suggest an autochthonous sources (algal or microbial) or photodegraded DOM[26–27].

The ranges of $S_{275–295}$, $S_{350–400}$ and S_R in the Oubangui system are comparable to that from other allochthonous dominated freshwater systems including temperate, Arctic, and tropical rivers[15,22,28–30]. The range of the a_{250}:a_{365} ratio is comparable to that from other temperate and Arctic rivers[15,28].

The large variations in stream S_R and a_{250}:a_{365} ratios that occurred along with changes in DOC concentrations and water discharge during the high flow period in the Oubangui River and its tributaries clearly indicate that DOM pools are being mobilized that are different than those typical of base flow conditions (Supplementary Tables 4 and 5). Similar changes in DOM optical properties across the hydrological cycle, especially in spectral slopes proxies, have also been reported in tropical[14,29] and Arctic rivers[28,30], as well as in an agricultural watershed in California[31]. Highest DOC concentrations were linked with lower S_R and a_{250}:a_{365} values, indicating an increase in the contribution of allochthonous sources to stream DOM due to greater surface runoff and leaching of organic rich layers during the high flow period[14,30]. However, lowest DOC concentrations were linked with higher S_R and a_{250}:a_{365} values, indicating that DOM is less aromatic in nature during the base flow period. This shift in DOM sources can be explained by the deepening of hydrologic flow paths through the soil profile and greater residences time of DOC in contact with soil subsurface microbial communities, leading to the mobilization of a more microbially processed DOM during base flow period[14,30]. However, combining optical and fluorescence properties of cDOM, Yamashita et al.[29] proposed another explanation in the

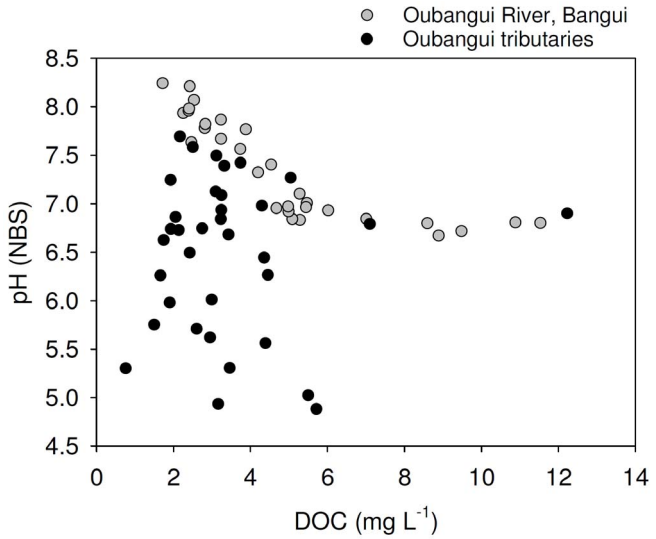

Figure 6 | Relationship between dissolved organic carbon (DOC) concentrations and in situ pH for the mainstem Oubangui (grey circles; data from 2 years of monitoring), and tributaries of the Oubangui (black circles).

interpretation of the increase of S_R during base flow period reported in tropical rivers in Venezuela. These authors suggested that the increase of S_R values could potentially result from a higher contribution of autochthonous source by enhanced plankton primary productivity during the low turbidity period. However, based on the previous study of Bouillon et al.[17], such autochthonous source has not been identified as contributor of DOC in the Oubangui River, supporting the hypothesis of a deepening of hydrological flow path as driver of changes in DOM sources.

The temporal variation observed in spectral slopes proxies in the Oubangui River are similar to those observed in the Epulu River[14]. During the wet period (April) the Epulu was characterized by lowest S_R values (0.834 ± 0.028) close to those measured in the Oubangui River during high flow period occurring from September to December (0.832 ± 0.041). In the Epulu River, S_R increased with decreasing discharge during post- and intermediary periods (November-February), with mean and maximal values of 0.962 ± 0.056 and 1.066, respectively. Mean value of S_R in the Oubangui River

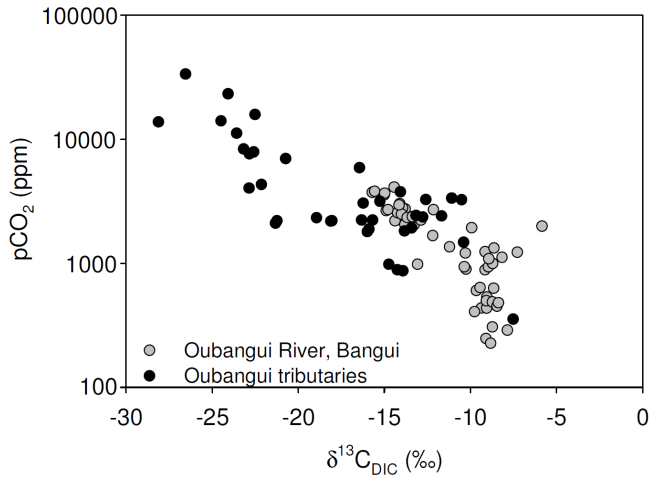

Figure 7 | Relationships between the carbon stable isotope composition of DIC ($\delta^{13}C_{DIC}$) and the partial pressure of CO_2 (pCO_2), for the mainstem Oubangui (grey circles; data from 2 years of monitoring), and tributaries of the Oubangui (black circles).

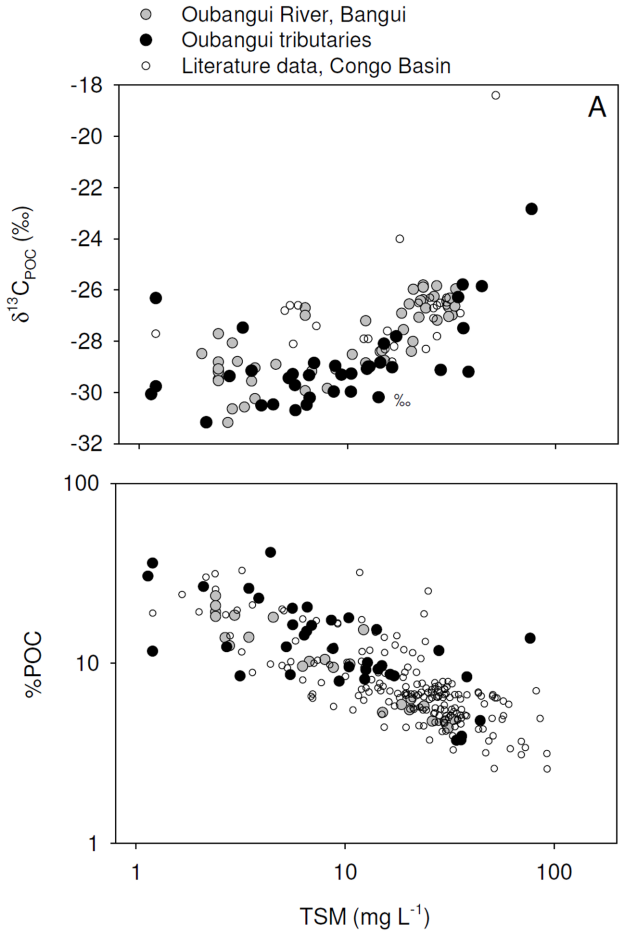

Figure 8 | Relationship between total suspended matter concentrations (TSM) and (a) $\delta^{13}C$ signatures of particulate organic carbon ($\delta^{13}C_{POC}$), and (b)the contribution of particulate organic carbon (POC) to the TSM pool (%POC) for the mainstem Oubangui, tributaries of the Oubangui and samples collected throughout the Congo basin (literature data from Mariotti et al. 1991, Sigha-Nkamdjou et al. 1993, Coynel et al. 2005, Bouillon et al. 2012, Spencer et al. 2012).

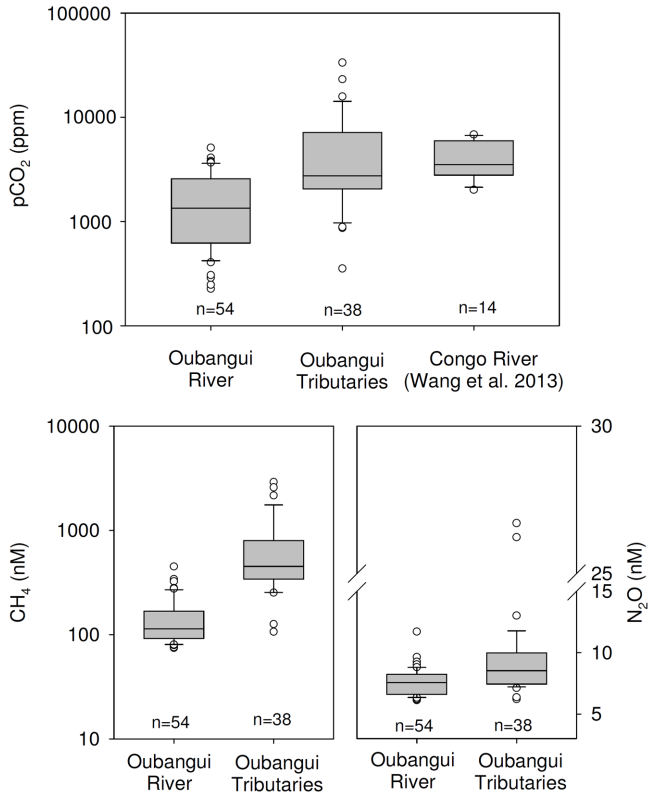

Figure 9 | Boxplots of data on pCO_2, CH_4, and N_2O concentrations for the mainstem Oubangui River (data from 2 years of monitoring), and tributaries of the Oubangui (all sites and sampling seasons combined). pCO_2 data for the lower Congo River are from Wang et al. (2013). *n* indicates the number of data points.

during base flow periods was higher, about 1.180 ± 0.116, with a maximal S_R value of 1.323. $S_{350-400}$ values showed the same temporal variations in both rivers, with lowest values in the Oubangui River compared to the Epulu River. The main difference between these two tropical rivers is the variations in $S_{275-295}$ values observed in the Oubangui River and to a lower extent in Oubangui tributaries. High flow period was associated with a clear decrease in $S_{275-295}$, whereas Spencer et al.[14] reported no seasonal variations in $S_{275-295}$ across the hydrological cycle.

Despite the similar temporal variations in DOC concentrations and DOM composition, spatial differences can be observed between the Oubangui River and its tributaries. The Oubangui River is characterized by a more important range of variations in whole cDOM parameters, including absorption coefficient, a_{250}:a_{365} (E2:E3), and spectral slope coefficients. This observation is quite different from those reported by Yamashita et al.[29], where hydrological changes seem to affect cDOM properties in tributaries to a larger extent than the main river channels.

$\delta^{13}C_{POC}$ values showed a positive correlation with sediment loads (Figure 8), but were generally in the range expected for C3-dominated catchments. The $\delta^{13}C$ values in the rivers draining the Ngotto Forest are relatively low (−32.2 to −29.1‰), but vegetation in these systems can be expected to have low $\delta^{13}C$ values given the effects of both high precipitation[32] and relatively closed-canopy structure (e.g.,[33]). The increasing pattern in $\delta^{13}C_{POC}$ values with increased sediment loads (albeit still low on a global scale, 34) suggests higher sediment inputs in catchments where C4 vegetation is more substantial (i.e., from savanna landscapes). The negative relationship between TSM loads and %POC (the contribution of POC to the total particulate matter load, Figure 8) has been previously observed in a range of individual river basins (e.g.,[35]), and on a global scale (e.g.,[4,36]). In our case, this correlation can be interpreted as reflecting the continuum from 2 contrasting end-members: (i) direct litter or organic-rich surface soil layers as observed in the majority of the rainforest rivers, and (ii) more soil-derived sediments as observed in the more turbid systems, with correspondingly lower %POC.

Inorganic carbon. HCO_3^- in rivers is mainly derived from the weathering of carbonate and silicate rocks, with the relative proportions depending to a very large extent on the lithology of the drainage basin[37–38]. Gaillardet et al. (39, based on data from 8) estimated the relative contributions of carbonate and silicate weathering to the bicarbonate load of the Congo River and some of its tributaries (Oubangui, Sangha, and Kasai) and found a contribution of silicate weathering generally between 50–60% except for the Sangha where carbonate dissolution dominated (only 9% resulting from silicate weathering). Since we do not have data on Cl^- concentrations as required in their approach, we used the simple stoichiometric model of Garrels and Mackenzie[37] whereby the contribution to TA from carbonate weathering (TA_{carb}) is computed from Ca^{2+} and Mg^{2+} concentrations and the contribution to TA from silicate weathering (TA_{sil}) is computed independently from dissolved silicon (Si) concentrations, according to:

$$TA_{carb} = 2*([Ca^{2+}] + [Mg^{2+}] - [SO_4^{2-}])$$

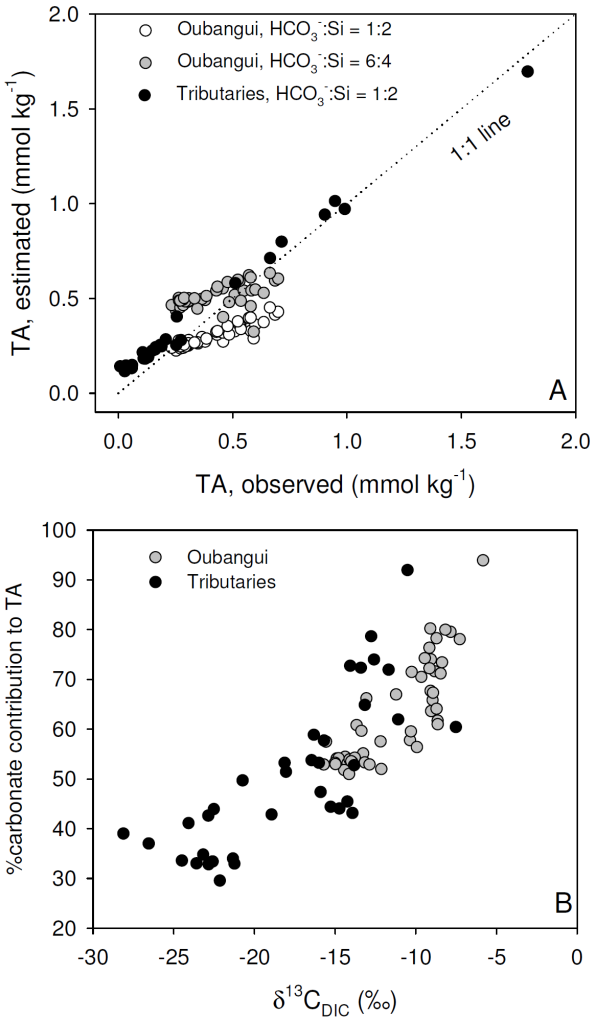

Figure 10 | Relationship between (A) observed and modeled total alkalinity (TA) (see text for details), and (B) the carbon stable isotope composition of DIC ($\delta^{13}C_{DIC}$) and the estimated contribution of TA derived from carbonate weathering to the observed TA.

$$TA_{sil} = [Si]/2$$

SO_4^{2-} allows to account for Ca^{2+} originating from the dissolution of gypsum ($CaSO_4$), but this correction term was ignored in absence of SO_4^{2-} data. In a companion study in the Tana basin (Kenya) we found SO_4^{2-} to correspond to about 10% of Ca^{2+} for a variety of streams and rivers[40], which is likely an upper estimate for our study area given the more humid climate and the absence of evaporative environments.

For the tributaries, there is a good linear regression between the modeled TA ($TA_{carb} + TA_{sil}$) and observed TA ($r^2 = 0.99$, $n = 36$, Figure 10A). In the Oubangui mainstem, the modeled TA is well correlated to the observed TA but markedly deviates from the 1:1 line as the values increase. The stoichiometric model of[37] assumes that the weathering of silicate rocks leads to a release of HCO_3^- and dissolved Si (DSi) according to a 1:2 ratio. This is true for common mineral forms such as olivine and albite, but the dissolution of some other mineral forms lead to a different HCO_3^-:DSi ratio. For instance, the weathering of plagioclase feldspar ($NaCaAl_3Si_5O_{16}$) leads to the release of HCO_3^- and DSi in a 6 : 4 ratio. While no detailed information is available on the mineralogy of the underlying bedrock in our study catchments, they are underlain mostly by metamorphic rocks in which feldspars are likely to be common consituents. When we apply this ratio to the Oubangui mainstem data, the recomputed modeled TA in the high values range is in better agreement with observed TA, than based on the HCO_3^-:DSi ratio of 1 : 2 (Figure 10A). The contribution of carbonate rock weathering (%TA_{carb}) was estimated as the percentage of TA_{carb} to total modeled TA ($TA_{carb} + TA_{sil}$), and ranged between 30% and 94%, encompassing the range of %TA_{carb} computed by Gaillardet et al.[39] between 40% and 91%. %TA_{carb} is positively correlated to TA indicating a lower contribution of carbonate rock weathering in the basins draining humid forest than savannah.

Carbon in HCO_3^- originating from silicate rock weathering comes exclusively from CO_2, while 1/2 of the C in HCO_3^- from carbonate rock comes from $CaCO_3$ and the other 1/2 from CO_2. If the CO_2 involved in the weathering comes from organic C degradation, $\delta^{13}C_{DIC}$ should have a negative signature (as indicated by the $\delta^{13}C$ signatures of DOC and POC), while marine $CaCO_3$ has a $\delta^{13}C$ signature close to 0‰[41].

This can explain the positive relationship between %TA_{carb} and $\delta^{13}C_{DIC}$ (Figure 10B). When applying a linear fit to these data (R^2=0.69), the extrapolated $\delta^{13}C_{DIC}$ values for the end members where the contribution of carbonate weathering is 0 and 100% are −31.3 and −1.5‰, respectively, which corresponds well with the expected values for terrestrial vegetation in the rainforest biome and marine carbonates. $\delta^{13}C_{DIC}$ values as low as those found in some of the Ngotto forest rivers (as low as −28.1‰) have, to the best of our knowledge, only been reported for a few rivers in the Amazon basin[42–43], and can only occur under conditions when alkalinity is extremely low and hence where silicate weathering dominates. The strong correlation between $\delta^{13}C_{DIC}$ and pCO_2 (Figure 7) on the one hand, and the link between $\delta^{13}C_{DIC}$ and carbonate weathering discussed above, suggest that the relative importance of silicate versus carbonate weathering may exert an important control on pCO_2 in the studied river systems. Such a mechanism is further suggested by the highly significant regressions ($p<0.0001$) between log(pCO_2) and the estimated contribution of carbonate weathering to TA (R^2=0.38), or with Si/Ca^{2+} ratios (R^2=0.35), i.e.,rock weathering would explain close to 35% of the variance of pCO_2. A recent analysis of factors controlling inorganic carbon speciation in North American rivers[44] concluded that while much of the variation in the spatial patterns of TA and pH can be explained by catchment processes and characteristics related to chemical weathering (e.g., precipitation, proportion of carbonate rocks), spatial variations in pCO_2 were mainly governed by in-river processes only indirectly related to the catchments (e.g. temperature through its effect on respiration). At the scale of our study, where factors such as temperature are much more homogeneous spatially and seasonally, it appears that the weathering regime could exert a partial control on the inorganic carbon speciation, and hence influence pCO_2 and water-atmosphere CO_2 exchange. It should be noted, however, that our calculated pCO_2 data from rivers with low pH are likely to be overestimates, since a comparison of calculated pCO_2 data with those measured in the field with a direct headspace technique suggests that the former approach induces a substantial bias towards higher pCO_2 under conditions of low pH (<6.5) and/or very low TA (Abril et al., in preparation). While this compromises some of the absolute pCO_2 data from rivers in the Ngotto forest, it is unlikely to distort the overall patterns described above.

Methane and nitrous oxide. The data compilation by Bastviken et al.[2] demonstrated the lack of CH_4 flux data from tropical systems, despite the fact that tropical freshwater systems are often claimed to show much higher CH_4 emissions than temperate or high-latitude systems. For the Oubangui tributaries, we have made no attempts to calculate diffusive CH_4 fluxes (due to the lack of data required to estimate gas exchange velocities, as outlined above for CO_2), yet it is evident that dissolved CH_4 concentrations are, on average, more than an order of magnitude higher than in the mainstem Oubangui River (Figure 9). Riverine CH_4 concentrations

in the few African catchments studied so far range drastically, with reported values between 1 and 6730 nM in the Athi-Galana-Sabaki River[45], between 48 and 870 nM in the Comoé, Bia and Tanoé rivers in Ivory Coast[46], and between 25 and 505 nM in the Tana River basin[47]. While CH_4 concentrations in the mainstem Oubangui show a pronounced seasonality (17, and Figure 2), a comparison of CH_4 data for the Lobaye and Mbaéré between our dry and wet season campaigns shows no distinct differences. While the riverine network is clearly a consistent source of CH_4 to the atmosphere, the data suggest that diffusive CH_4 fluxes are highly variable in space and time and therefore difficult to upscale reliably. As reported earlier for the mainstem Oubangui River, dissolved N_2O levels were generally low (6.4–13.0 nM, except for the Kélé, a small and shallow rainforest stream draining into the Mbaére where N_2O concentrations reached 26.7 and 26.2 nM during the 2012 and 2013 sampling campaigns, respectively). These values represent only a slight oversaturation with respect to atmospheric equilibrium (137 ± 22%, 380–402% for the Kélé). A synthesis by Baulch et al.[48] found higher N_2O emissions to be associated with increasing N inputs, hence the low N_2O concentrations observed are in line with the pristine status of our study catchments and the observed low nitrate levels (median of 7.1 μM, range: 0–50 μM, n= 32; own unpublished data).

Concluding remarks. Overall, our results demonstrate that even within a relatively small set of subcatchments of the Oubangui River, biogeochemical characteristics of different rivers and streams show highly contrasting characteristics on the one hand, yet consistent co-variations between parameters on the other hand. According to Raymond et al.[3] and Regnier et al.[49], one of the factors limiting our ability to better constrain the role of rivers in regional and global C budgets is that the current empirical database is too sparse to adequately resolve the diversity of soil types, inland waters, estuaries and coastal systems, and specifies the Congo Basin as one of the key areas of regional priority. The data collected and compiled here, while covering only a small subset of the Congo Basin, suggest that large data collection efforts will be required to adequately describe the aquatic biogeochemical variability for this large tropical basin. However, the systematic co-variation between some of the examined proxies of C origin and transformation, and the apparent link with certain catchment characteristics (lithology and vegetation) provide some important clues on the type of classification and characterization needed to upscale future data to the catchment scale.

Methods

The Oubangui River (Figure 1) is the second largest tributary of the Congo River (after the Kasai), with a length of 2400 km from the source (Uele River) to its confluence with the Congo River, and a drainage basin of 644000 km^2, of which 489000 km^2 (76%) is located upstream of Bangui[10]. The Oubangui catchment upstream of Bangui is dominated by dry wooded savannahs, with more humid forest situated downstream towards the confluence with the Congo mainstem. The mean annual precipitation in the catchment is ~1400–1540 mm y^{-1} [10]. The hydrological cycle of the Oubangui is characterized by a single main flood peak and maximum discharge typically in October-November. Annual discharge has fluctuated between 2120 $m^3 s^{-1}$ (1990) and 6110 $m^3 s^{-1}$ (1969). Although we did not find land-use data specifically for the Oubangui catchment, deforestation rates in the CAR are reported to be among the lowest in Africa (net deforestation of 0.06% y^{-1} [50]). According to the Food and Agriculture Organisation (FAO) statistics (http://faostat.fao.org/), agricultural land use has remained stable between 1961 and 2010, and makes for ~8% of the total land area. Considering a national population density of ~7 inhabitants km^{-2}, these figures support classifying the Oubangui catchment as nearly pristine. Monitoring on the Oubangui in the city of Bangui (CAR, 4°21′ N, 18° 34′ E) was initiated in late March 2010, and was followed by approximately 2-weekly sampling. A subset of data collected between March 2010 and March 2011 were presented in[21]; data on the subsequent year of monitoring (after which this programme ended) are included here.

Tributaries of the Oubangui were sampled in March 2010 (dry season), March 2011 (dry season), and November 2012 (wet season). During the first field campaign, two sites were sampled along the Mbali River (Fig. 1), as well as the Mpoko River just south of Bangui (see also 13), and the main rivers draining the Ngotto Forest, Lobaye province (Fig. 1). The Ngotto Forest was revisited in 2011 and 2012 for more extensive sampling on the main rivers (Mbaéré, Lobaye, and Bodingué) and some of their minor tributaries. The Ngotto Forest, bordering on the Republic of Congo (a.k.a. Congo Brazzaville) and characterized by annual precipitation of ~1600 mm, is classified as a semi-deciduous rainforest and lies south of the wooded savannahs of the Guinea-Sudanian transition zone. Water levels were lower during the dry season surveys (March) than during the wet season (November), but water level differences are rather small (1.0–1.5 m), in line with the relatively stable discharge of the Lobaye River (monthly average flow ranging between 250 and 500 m^3 s-1 for the period 1950–1984; data from the Global River Discharge Database (http://www.sage.wisc.edu/riverdata/, accessed February 2014). The Mbaéré and Bodingué are the two main permanent rivers, which are bordered by extensive areas of seasonally flooded forests. The Bodingué River joins the Mbaéré River prior to joining the Lobaye River, which lies on the northern side of the Ngotto Forest and represents the border towards drier, savannah landscapes to the North. The Lobaye River is an important tributary of the Oubangui River. The Ngotto Forest forms a protected area with high biodiversity, and very low human population densities[51]. The geology of the region is complex and includes igneous, metamorphic, and Mesoproterozoic– Neoproterozoic sedimentary formations that include calcareous sediments[52].

Water temperature, conductivity, dissolved oxygen (O_2) and pH were measured in situ with a YSI ProPlus multimeter, whereby the O_2 and pH probes were calibrated on each day of data collection using water saturated air and United States National Bureau of Standards buffer solutions (4 and 7), respectively. All sampling for larger rivers was performed from dugout canoes at ~0.5 m below the water surface, in a few cases sampling was performed from a bridge (Mpoko) or from the river shore (Mbali). Samples for dissolved gases (CH_4, N_2O) and the stable isotope composition of dissolved inorganic C ($\delta^{13}C_{DIC}$) were collected with a Niskin bottle or a custom-made sampling bottle consisting of an inverted 1L polycarbonate bottle with the bottom removed, and ~0.5 m of tubing attached in the screw cap[53]. 12 mL exetainer vials (for $\delta^{13}C_{DIC}$) and 50 mL serum bottles (for CH_4 and N_2O) were filled from water flowing from the outlet tubing, poisoned with HgCl2, and capped without headspace. Approximately 2000 mL of water were collected 0.5 m below the water surface for other particulate and dissolved variables, and filtration and sample preservation was performed in the field within 2 h of sampling.

Samples for total suspended matter (TSM) were obtained by filtering 200–1000 mL of water on pre-combusted (4 h at 500°C) and pre-weighed glass fiber filters (47 mm GF/F, 0.7 μm nominal pore size), and dried in ambient air during the fieldwork. Samples for determination of particulate organic C (POC), particulate nitrogen (PN) and C isotope composition of POC ($\delta^{13}C_{POC}$) were collected by filtering 50–300 mL of water on pre-combusted 25 mm GF/F filters (0.7 μm nominal pore size). The filtrate from the TSM filtrations was further filtered on 0.2 μm polyethersulfone syringe filters (Sartorius, 16532-Q) for total alkalinity (TA), DOC and $\delta^{13}C_{DOC}$ (8–40 mL glass vials with Polytetrafluoroethylene coated septa). TA was analysed by automated electro-titration on 50 mL samples with 0.1 mol L^{-1} HCl as titrant (reproducibility estimated as typically better than ± 3 μmol kg^{-1} based on replicate analyses). The partial pressure of CO_2 (pCO_2) and DIC concentrations were computed from pH and TA measurements using thermodynamic constants of Millero[54] as implemented in the CO2SYS software[55]. It should be noted, however, that this approach is expected to overestimate pCO_2 in some of the blackwater rivers (see Discussion).

For the monitoring data on the Oubangui River, CO_2 exchange with the atmosphere was calculated as F= kαΔpCO2 where k is the gas transfer velocity, α is the solubility coefficient for CO2, and ΔpCO2 represents the difference in partial pressure of CO_2 between water and air. Monthly averages corresponding to time of sampling of atmospheric pCO_2 from Mount Kenya (Kenya, -0.05°N 37.80°E) were retrieved GLOBALVIEW-CO2 database (Carbon Cycle Greenhouse Gases Group of the National Oceanic and Atmospheric Administration, Earth System Research Laboratory). k values were calculated using two approaches, one based on the relationship between wind speed and k600 (i.e., k normalized to a constant temperature of 20°C), and an alternative approach using a gas transfer parameterization based on depth and water current that was developed for rivers and streams; details can be found in Bouillon et al.[17]. No CO_2 flux estimates were made for the tributary sampling sites, since both approaches would be hampered by a lack of adequate ancillary information - data on river depth and flow velocity are lacking, and the varying degree of canopy closure would compromise the use of modeled wind speed data.

For the analysis of $\delta^{13}C_{DIC}$, a 2 ml helium (He) headspace was created, and H_3PO_4 was added to convert all DIC species to CO_2. After overnight equilibration, part of the headspace was injected into the He stream of an elemental analyser – isotope ratio mass spectrometer (EA-IRMS, ThermoFinnigan Flash HT and ThermoFinnigan DeltaV Advantage) for $\delta^{13}C$ measurements. The obtained $\delta^{13}C$ data were corrected for the isotopic equilibration between gaseous and dissolved CO_2 as described in Gillikin and Bouillon[56] and measurements were calibrated with certified reference materials LSVEC and either NBS-19 or IAEA-CO-1. Reproducibility of $\delta^{13}C$ measurements was 0.2‰ or better. Concentrations of CH_4 and N_2O were determined via the headspace equilibration technique (20 mL N_2 headspace in 50 mL serum bottles) and measured by gas chromatography (GC, 63) with flame ionization detection (GC-FID) and electron capture detection (GC-ECD) with a SRI 8610C GC-FID-ECD calibrated with CH_4:CO_2:N_2O:N_2 mixtures (Air Liquide Belgium) of 1, 10 and 30 ppm CH_4 and of 0.2, 2.0 and 6.0 ppm N_2O, and using the solubility coefficients of Yamamoto et al.[57] for CH_4 and Weiss and Price[58] for N_2O.

25 mm filters for POC, PN and $\delta^{13}C_{POC}$ were decarbonated with HCl fumes for 4 h, re-dried and packed in Ag cups. POC, PN, and $\delta^{13}C_{POC}$ were determined on the

abovementioned EA-IRMS using the thermal conductivity detector (TCD) signal of the EA to quantify POC and PN, and by monitoring m/z 44, 45, and 46 on the IRMS. An internally calibrated acetanilide and sucrose (IAEA-C6) were used to calibrate the $\delta^{13}C_{POC}$ data and quantify POC and PN, after taking filter blanks into account. Reproducibility of $\delta^{13}C_{POC}$ measurements was better than ±0.2‰. Samples for DOC and $\delta^{13}C_{DOC}$ were analysed either on a Thermo HiperTOC-IRMS, or with an Aurora1030 TOC analyser (OI Analytical) coupled to a Delta V Advantage IRMS. Typical reproducibility observed in duplicate samples was in most cases $<\pm5\%$ for DOC, and ±0.2‰ for $\delta^{13}C_{DOC}$. For a subset of samples from the Ngotto Forest, we compared DOC concentrations and $\delta^{13}C$ data for samples filtered on 0.2 µm (as described above) and only on 0.7 µm GF/F filters; for both variables no significant differences were found ($n=15$, two-tailed paired t-test, in both cases $p<0.0001$ at 95% confidence interval, data in Supplementary Table 1).

Samples for major element concentrations and Si were filtered through a 0.45 µm polyethersulfone (PES) or polycarbonate (PC) filter, and measured by ICP-AES (Iris Advantage, Thermo) or ICP-MS (Perkin Elmer Elan 6100).

Samples for the analyses of cDOM spectral characteristics were prepared similarly as for DOC analyses, but without H_3PO_4 addition. cDOM samples were stored in amber glass vials with PTFE-coated septa. Absorbance measurements were recorded on a Perkin-Elmer UV/Vis 650S using a 1 cm quartz cuvette. Absorbance spectra were measured from 190 to 900 nm at 1 nm increments and noise instrument was assessed measuring Milli-Q water as blank. The correction for scattering, index of refraction and blank was performed by fitting the absorption spectra to the data over the range 200–700 nm according to the following equation:

$$A_\lambda = A_0 e^{-S(\lambda-\lambda_0)} + K, \quad (1)$$

where A_λ and A_0 are the absorbance measured at defined wavelength λ (nm) and at reference wavelength $\lambda_0=375$ nm, respectively, S is the spectral slope (nm^{-1}) that describes the approximate exponential decline in absorption with increasing wavelength, and K is a background offset. According to Johannessen and Miller[59], the offset value was then subtracted from the whole spectrum. The fit was not used for any purpose other than to provide an offset value. After correction, absorption coefficients were calculated according to the relation:

$$a_\lambda = 2.303 \times A_\lambda / L, \quad (2)$$

where aλ is the absorption coefficient (m^{-1}) at wavelength λ, A is the absorbance corrected at wavelength λ, and L the path length of the optical cell in meters (0.01 m).

Several optical indices were calculated to investigate CDOM properties, including spectral slopes over the ranges 275–295 nm ($S_{275-295}$) and 350–400 nm ($S_{350-400}$), the slope ratio (SR) and the a_{250}:a_{365} ratio. Spectral slopes were determined using linear regression for the log-transformed a spectra for the intervals 275–295 nm and 350–400 nm and the slope ratio SR was calculated as the ratio of $S_{275-295}$ to $S_{350-400}$[22]. The a_{250}:a_{365} ratio (also called E2:E3 ratio) was calculating using absorption coefficients at the appropriate wavelengths.

Literature data on specific parameters were obtained either from tabulated values in the relevant papers, data supplied by authors, or digitized from figures using PlotDigitizer v2.6.1 (http://plotdigitizer.sourceforge.net/).

1. Cole, J. J. *et al.* Plumbing the global carbon cycle: Integrating inland waters into the terrestrial carbon budget. *Ecosystems* **10**, 171–184 (2007).
2. Bastviken, D. *et al.* Freshwater methane emissions offset the continental carbon sink. *Science* **33**, 50 (2011).
3. Raymond, P. A. *et al.* Global carbon dioxide emissions from inland waters. *Nature* **503**, 355–359 (2013).
4. Ludwig, W., Probst, J. L. & Kempe, S. Predicting the oceanic input of organic carbon by continental erosion. *Global Biogeochem. Cycles* **10**, 23–41 (1996).
5. Schlünz, B. & Schneider, R. R. Transport of terrestrial organic carbon to the oceans by rivers: re-estimating flux and burial rates. *Int. J. Earth Sci.* **88**, 599–606 (2000).
6. Aufdenkampe, A. K. *et al.* Riverine coupling of biogeochemical cycles between land, oceans, and atmosphere. *Front. Ecol. Environ.* **9**, 53–60 (2011).
7. Probst, J. L., Mortatti, J. & Tardy, Y. Carbon river fluxes and weathering CO_2 consumption in the Congo and Amazon river basins. *Appl. Geochem.* **9**, 1–13 (1994).
8. Négrel, P. *et al.* Erosion sources determined by inversion of major and trace element ratios and strontium isotopic ratios in river water: the Congo Basin case. *Earth Planet. Sci. Lett.* **120**, 59–79 (1993).
9. Seyler, P. & Elbaz-Poulichet, F. Biogeochemical control on the temporal variability of trace element concentrations in the Oubangui river (Central African Republic). *J. Hydrol.* **180**, 319–332 (1996).
10. Coynel, A. *et al.* Spatial and seasonal dynamics of total suspended sediment and organic carbon species in the Congo River. *Glob. Biogeochem. Cycles* **19**, GB4019 (2005).
11. Laraque, A. *et al.* A review of material transport by the Congo River and its tributaries. *Hydrol. Process.* **23**, 3216–3224 (2009).
12. Seyler, P. *et al.* Concentrations, fluctuations saisonnières et flux de carbonne dans le bassin du Congo. *Grands Bassins Fluviaux* (ORSTOM, Paris, 1995).
13. Mariotti, A. *et al.* Carbon isotope composition and geochemistry of particulate organic matter in the Congo River (Central Africa): application to the study of Quaternary sediments off the mouth of the river. *Chem. Geol.* **86**, 345–357 (1991).
14. Spencer, R. G. M. *et al.* Temporal controls on dissolved organic matter and lignin biogeochemistry in a pristine tropical river, Democratic Repblic of Congo. *J. Geophys. Res.* **115**, G03013, doi:10.1029/2009JG001180 (2010).
15. Spencer, R. G. M. *et al.* An initial investigation into the organic matter biogeochemistry of the Congo River. *Geochim. Cosmochim. Acta* **84**, 614–627 (2012).
16. Wang, Z. A. *et al.* Inorganic carbon speciation and fluxes in the Congo River. *Geophys Res Lett* **40**, doi: 10.002/grl.50160 (2013).
17. Bouillon, S. *et al.* Organic matter sources, fluxes and greenhouse gas exchange in the Oubangui River (Congo River basin). *Biogeosciences* **9**, 2045–2062; doi:10.5194/bg-9-2045-2012 (2012).
18. Laraque, A. *et al.* Impact of lithological and vegetal covers on flow discharge and water quality of Congolese tributaries of the Congo River. *Rev. Sci. Eau* **11**, 209–224 (1998).
19. Mann, P. J. *et al.* The biogeochemistry of carbon across a gradient of streams and rivers within the Congo Basin. *J. Geophys. Res.* doi:10.1002/2013JG002442 (in press).
20. Richey, J. E. *et al.* Outgassing from Amazonian rivers and wetlands as a large tropical source of atmospheric CO_2. *Nature* **416**, 617–620 (2002).
21. Mayorga, E. & Aufdenkampe, A. [Processing of bioactive elements in the Amazon River system]. *The Ecohydrology of South American Rivers and Wetlands* [McClain, M.E. (ed)] [1–24](IAHS Press, Wallingford, UK, 2002).
22. Helms, J. R. *et al.* Absorption spectral slopes and slope ratios as indicators of molecular weight, source, and photobleaching of chromophoric dissolved organic matter. *Limnol. Oceanogr.* **53**, 955–969 (2008).
23. Peuravuori, J. & Pihlaja, K. Molecular size distribution and spectroscopic properties of aquatic humic substrances. *Anal. Chim. Acta* **337**, 133–149 (1997).
24. Spencer, R. G. M., Butler, K. D. & Aiken, G. R. Dissolved organic carbon and chromophoric dissolved organic matter properties of rivers in the USA. *J. Geophys. Res.* **117**, G03001, doi:10.1029/2011JG001928 (2012).
25. Aiken, G. R. *et al.* Isolation of hydrophobic organic-acids from water using nonionic macroporous resins. *Org. Geochem.* **18**, 567–573 (1992).
26. McKnight, D. M. & Aiken, G. R. [Sources and age of aquatic humus]. *Aquatic Humic Substances* [Hessen, D. & TranvikL. (eds)] [9–39] (Springer, Berlin, 1998).
27. Cory, R. M. *et al.* Chemical characteristics of fulvic acids from Arctic surface waters:Microbial contributions and photochemical transformations. *J. Geophys. Res.* **112**, G04S51, doi:10.1029/2006JG000343 (2007).
28. Spencer, R. G. M. *et al.* Utilizing chromophoric dissolved organic matter measurements to derive export and reactivity of dissolved organic carbon exported to the Arctic Ocean: A case study of the Yukon River, Alaska. *Geophys. Res. Lett.* **36**, L06401, doi:10.1029/2008GL036831 (2009).
29. Yamashita, Y. *et al.* Optical characterization of dissolved organic matter in tropical rivers of the Guayana Shield, Venezuela. *J. Geophys. Res.* **115**, G00F10, doi:10.1029/2009JG000987 (2010).
30. Mann, P. J. *et al.* Controls on the composition and lability of dissolved organic matter in Siberia's Kolyma River basin. *J. Geophys. Res.* **117**, G01028, doi:10.1029/2011JG001798 (2012).
31. Hernes, J. P. *et al.* The role of hydrologic regimes on dissolved organic carbon composition in an agricultural watershed. *Geochim. Cosmochim. Acta* **72**, 5266–5277 (2008).
32. Kohn, M. J. Carbon isotope compositions of terrestrial C3 plants as indicators of (paleo)ecology and (paleo)climate. *PNAS* **107**, 19691–19695 (2010).
33. Cerling, T. E., Hart, J. A. & Hart, T. B. Stable isotope ecology of the Ituri Forest. *Oecologia* **138**, 5–12 (2004).
34. Milliman, D. J. & Farnsworth, L. K. *River discharge to the coastal ocean: a global synthesis* (Cambridge University Press, 2011).
35. Tamooh, F. *et al.* Distribution and origin of suspended matter and organic carbon pools in the Tana River Basin, Kenya. *Biogeosciences* **9**, 2905–2920; DOI:10.5194/bg-9-2905-2012 (2012).
36. Meybeck, M. Carbon, nitrogen, and phosphorus transport by world rivers. *Am. J. Sci.* **282**, 401–450 (1982).
37. Garrels, R. M. & Mackenzie, F. T. *Evolution of Sedimentary Rocks* (W.W. Norton, New York, 1971).
38. Meybeck, M. Global chemical weathering of surficial rocks estimated from river dissolved loads. *Am. J. Sci.* **287**, 401–428 (1987).
39. Gaillardet, J., Dupré, B. & Allègre, C. J. A global mass budget applied to the Congo Basin rivers: erosion rates and continental crust composition. *Geochim. Cosmochim. Acta* **59**, 3469–3485 (1995).
40. Tamooh, F. *et al.* Dynamics of dissolved inorganic carbon and aquatic metabolism in the Tana River Basin, Kenya. *Biogeosciences* **10**, 6911–6928; DOI:10.5194/bg-10-6911-2013 (2013).
41. Mook, W. G. & Tan, F. C. [Stable carbon isotopes in rivers and estuaries]. *Biogeochemistry of Major World Rivers* [Degens, E.T., Kempe, S. & Richey, J.E. (eds)] [245–264] (John Wiley, Hoboken, N. J., 1991).
42. Mayorga, E. *et al.* Young organic matter as a source of carbon dioxide outgassing from Amazonian rivers. *Nature* **436**, 538–541 (2005).
43. Ellis, E. E. *et al.* Factors controlling water-column respiration in rivers of the central and southwestern Amazon Basin. *Limnol. Oceanogr.* **57**, 527–540 (2012).
44. Lauerwald, R. *et al.* What controls the spatial patterns of the riverine carbonate system? A case study for North America. *Chem. Geol.* **337–338**, 114–127 (2013).

45. Marwick, T. R. *et al.* Dynamic seasonal nitrogen cycling in response to anthropogenic N-loading in a tropical catchment, the Athi-Galana-Sabaki River, Kenya. *Biogeosciences* **11**, 443–460; DOI:10.5194/bg-11-443-2014 (2014).
46. Koné, Y. J. M. *et al.* Seasonal variability of methane in the rivers and lagoons of Ivory Coast (West Africa). *Biogeochemistry* **100**, 21–37 (2010).
47. Bouillon, S. *et al.* Distribution, origin and cycling of carbon in the Tana River (Kenya): a dry season basin-scale survey from headwaters to the delta. *Biogeosciences* **6**, 2475–2493; DOI:10.5194/bg-6-2475-2009 (2009).
48. Baulch, H. M. *et al.* Nitrogen enrichment and the emissons of nitrous oxide from streams. *Glob. Biogeochem. Cycles* **25**, GB4013 (2011).
49. Regnier, P. *et al.* Anthropogenic perturbation of the carbon fluxes from land to ocean. *Nature Geosc* **6**, 597–607 (2013).
50. Duveiller, G. *et al.* Deforestation in Central Africa: estimates at regional, national and landscape levels by advanced processing of systematically-distributed Landsat extracts. *Remote Sens. Environm.* **112**, 1969–1981 (2008).
51. Brugière, D., Sakom, D. & Gautier-Hion, A. The conservation significance of the proposed Mbaéré-Bodingué national park, Central African Republic, with special emphasis on its primate community. *Biodiversity and Conservation* **14**, 505–522 (2005).
52. Milesi, J. P. *et al.* An overview of the geology and major ore deposits of Central Africa: Explanatory note for the 1:4,000,000 map "Geology and major ore deposits of Central Africa". *J. Afr. Earth Sci.* **44**, 571–595 (2006).
53. Abril, G., Commarieu, M. V. & Guérin, F. Enhanced methane oxidation in an estuarine turbidity maximum. *Limnol. Oceanogr.* **52**, 470–475 (2007).
54. Millero, F. J. The thermodynamics of the carbonic acid system in seawater. *Geochim. Cosmochim. Acta* **43**, 1651–1661 (1979).
55. Lewis, E. & Wallace, D. W. R. *Program developed for CO_2 system calculations* (Carbon Dioxide Information Analysis Center, Oak Ridge National Laboratory, U.S. Department of Energy, Oak Ridge, Tennessee, 1998). Available online at http://cdiac.ornl.gov/oceans/co2rprt.html, accessed February 2014.
56. Gillikin, D. P. & Bouillon, S. Determination of $\delta^{18}O$ of water and $\delta^{13}C$ of dissolved inorganic carbon using a simple modification of an elemental analyzer – isotope ratio mass spectrometer (EA-IRMS): an evaluation. *Rapid Comm. Mass Spectrom.* **21**, 1475–1478 (2007).
57. Weiss, F. R. & Price, B. A. Nitrous oxide solubility in water and seawater. *Mar. Chem.* **8**, 347–359 (1980).
58. Yamamoto, S., Alcauskas, J. B. & Crozier, T. E. Solubility of methane in distilled water and seawater. *J. Chem. Eng. Data* **21**, 78–80 (1976).
59. Johannessen, S. C. & Miller, W. L. Quantum yield for the photochemical production of dissolved inorganic carbon in seawater. *Mar. Chem.* **76**, 271–283 (2001).

Acknowledgments

This work was financially supported by the European Research Council (StG 240002: AFRIVAL: "African river basins: catchment-scale carbon fluxes and transformations"), two travel grants to S.B. from the Research Foundation Flanders (FWO-Vlaanderen), and a National Geographic Society Research and Exploration Grant (#8885-11) to D.P.G. and S.B. We thank Marc-Vincent Commarieu for analyses of TA, Zita Kelemen for IRMS support, Harold Hughes (Museum for Central Africa, Tervuren, Belgium) and Kristin Coorevits (KU Leuven) for ICP-MS analyses, and Christiane Lancelot for access to the Perkin-Elmer UV/Vis 650S. A.V.B. and T.L. are a senior research associate and postdoctoral researcher, respectively, with the Fonds National de la Recherche Scientifique (FNRS, Belgium). We thank all staff members of the ECOFAC (Ecosystemes Forestiers d'Afrique Centrale) centre in Ngotto for their hospitality and assistance in the field, in particular Denis Passy. A. Coynel and A. Wang kindly provided the raw data of their published work. J. Hartmann and Nils Moosdorf kindly shared their knowledge concerning the lithology of the study catchments.

Author contributions

S.B. and A.V.B. designed the research; S.B., A.Y. and D.P.G. conducted the field sampling, S.B., A.V.B., T.L., C.T. and F.D. analysed samples, S.B. drafted the manuscript with input from A.V.B., A.Y., D.P.G., T.L., C.T. and F.D.

Additional information

Supplementary information accompanies this paper at http://www.nature.com/scientificreports

Competing financial interests: The authors declare no competing financial interests.

How to cite this article: Bouillon, S. *et al.* Contrasting biogeochemical characteristics of the Oubangui River and tributaries (Congo River basin). *Sci. Rep.* **4**, 5402; DOI:10.1038/srep05402 (2014).

Supplementary material.

Contrasting biogeochemical characteristics of the Oubangui River and tributaries(Congo River basin).

Steven Bouillon, Athanase Yambélé, David P. Gillikin, Cristian Teodoru, François Darchambeau, Thibault Lambert, and Alberto V. Borges.

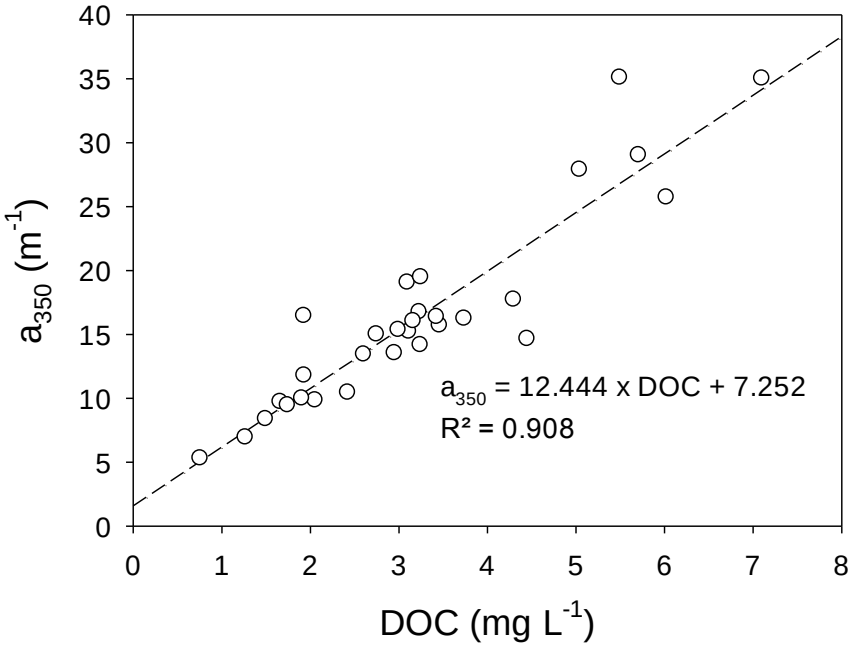

Figure S1: Relationship between DOC concentrations and a_{350} for all sites in the Oubangui tributaries sampled in 2012 and 2013. This relationship was used to estimate DOC concentrations and the annual flux of DOC in the mainstam Oubangui for the 2nd year of monitoring, when no direct DOC measurements are available. The relationship shown here is consistent with other data collected throughout the Congo basin (own unpublished data).

Supplementary Table 1: Comparison of concentrations and $\delta^{13}C$ signatures of dissolved organic carbon (DOC) on samples prepared by (i) immediately preserving samples filtered through 0.7 µm GF/F filters, and (ii) preservation after further filtration through 0.2 µm syringe filters. No significant differences were found for either DOC concentrations or $\delta^{13}C_{DOC}$ (paired t-test).

Site (March 2011 samples)	[DOC], 0.2 µm	[DOC], 0.7 µm	$\delta^{13}C_{DOC}$, 0.2 µm	$\delta^{13}C_{DOC}$, 0.7 µm
Imbalataka (tributary of Mbaéré)	1.27	1.40	-29.9	-30.0
Mbaéré	1.50	1.54	-29.7	-29.0
Mbaéré	1.66	1.74	-29.9	-29.6
Kélé (tributary of Mbaéré)	4.45	4.41	-30.2	-30.3
Lubé (left bank tributary of Lobaye)	5.50	5.46	-27.1	-26.4
Lobaye	1.93	1.76	-28.2	-28.7
Mamboussou (right bank tributary of Lobaye)	12.23	12.10	-29.2	-29.1
Lobaye	2.06	1.98	-28.6	-28.6
Ibéléké (right bank tributary of Lobaye)	3.24	3.29	-29.7	-29.8
Mbaéré, after confluence with Bodingué	2.42	2.32	-30.0	-29.8
Lobaye, dowstream of confluence with Mbaéré	1.90	1.89	-29.0	-29.0
Lobaye	1.74	1.72	-27.3	-28.3
Lobaye	1.93	2.00	-28.7	-28.4
Bodingué	4.30	4.29	-30.1	-30.0
Mbaéré, after confluence with Bodingué	3.46	3.50	-29.9	-29.9

Supplementary Table 2 : Full dataset on physico-chemical and biogeochemical data collected on the mainstem Oubangui River between April 2011 and March 2012.

Date	Discharge (m^3 s-1)	T (°C)	$\%O_2$	Specific conductivity ($\mu S\ cm^{-1}$)	pH (NBS scale)	TSM ($mg\ L^{-1}$)	δ^{13}C-DIC (‰)	POC ($mg\ L^{-1}$)	PN ($mg\ L^{-1}$)	POC/PN (weight)	%POC
14/04/2011	421	29.3		72.3	7.85	2.4	-8.7	0.462	0.060	7.7	19.3
28/04/2011	505	30.0		74.1	7.93	3.0	-7.8	0.548	0.069	7.9	18.5
14/05/2011	717	30.2	115.1	67.0	8.00	4.5		0.816	0.101	8.1	18.0
28/05/2011	859	30.1	97.8	63.4	8.23	12.3	-5.8	1.884	0.293	6.4	15.4
16/06/2011	1180	29.9	97.1	60.0	7.52	8.0	-7.3	0.839	0.122	6.9	10.5
28/06/2011	1395	29.6	93.9	53.8	7.32	8.8	-9.1	0.835	0.125	6.7	9.5
13/07/2011	1214	28.9	90.2	49.2	7.48	6.7	-13.1	0.690	0.102	6.8	10.2
30/07/2011	1377	29.6	96.5	44.0	7.44	10.6		1.043	0.142	7.4	9.9
13/08/2011	2046	28.2	94.4	41.5	7.25	20.3	-11.2	1.122	0.178	6.3	5.5
30/08/2011	3206	28.6	72.4	37.7	6.96	30.7	-13.7	1.399	0.190	7.4	4.6
10/09/2011	3528	28.1	72.3	35.1	6.89	32.9	-13.4	1.604	0.172	9.3	4.9
25/09/2011	4602	28.4	72.0	35.0	6.75	30.1	-15.6	1.422	0.161	8.8	4.7
15/10/2011	6266	27.8	84.2	32.1	6.69	31.2	-14.4	1.365	0.138	9.9	4.4
29/10/2011	7688	27.2	85.3	31.3	6.72	26.1	-15.0	1.246	0.121	10.3	4.8
12/11/2011	7128	28.2	83.0	30.8	6.56	23.9		1.380	0.136	10.2	5.8
26/11/2011	5725	28.0	87.6	30.6	6.80	18.7	-14.1	1.102	0.106	10.4	5.9
10/12/2011	3432	26.9	92.5	31.9	6.86	20.7	-12.1	1.313	0.139	9.4	6.3
24/12/2011	1972	27.4	93.0	35.6	7.07	15.1	-9.9	0.808	0.118	6.8	5.3
14/01/2012	1248	25.1	98.0	40.7	7.28	6.3	-8.6	0.603	0.091	6.6	9.6
28/01/2012	922	27.1	99.5	45.5	7.47	2.7	-8.7	0.370	0.059	6.2	13.9
11/02/2012	654	28.4	96.5	51.4	7.48	2.8	-8.9	0.350	0.055	6.4	12.5
24/02/2012	544	29.3	99.0	56.2	7.91	3.5	-8.5	0.483	0.075	6.5	13.9
10/03/2012	401	29.3	99.7	61.9	7.92	2.4	-8.4	0.437	0.072	6.1	18.2
31/03/2012	293	29.1	96.2	71.1	7.62	2.4	-8.2	0.501	0.084	6.0	20.9

Supplementary Table 2 (continued)

Date	δ^{13}C-POC (‰)	TA (mmol L^{-1})	DIC (mmol L^{-1})	pCO_2 (ppm)	N_2O (nmol L^{-1})	CH_4 (nmol L^{-1})	Ca (µM)	Mg (µM)	Si (µM)
14/04/2011	-29.2	0.686	0.696	487	7.2	126.7	162.0	123.0	180.0
28/04/2011	-28.8	0.699	0.699	289	8.5	138.5	170.7	124.3	175.4
14/05/2011	-28.9	0.636	0.676	1373	6.4	341.3	148.5	111.5	154.7
28/05/2011	-27.2	0.592	0.651	1990	7.3	450.6	135.9	105.4	35.1
16/06/2011	-29.8	0.536	0.572	1226	6.6	324.5	132.2	100.1	148.3
28/06/2011	-29.1	0.485	0.521	1239	6.4	261.8	111.7	89.4	171.5
13/07/2011	-29.2	0.429	0.458	981	6.7	234.1	107.0	70.4	218.8
30/07/2011	-28.5	0.366	0.393	935	6.2	230.4	97.4	61.1	202.1
13/08/2011	-28.4	0.346	0.388	1356	8.4	187.5	89.9	55.4	177.4
30/08/2011	-27.0	0.308	0.380	2341	11.7	147.0	85.3	48.1	219.6
10/09/2011	-26.6	0.265	0.339	2379	9.3	122.4	82.9	42.3	224.3
25/09/2011	-26.4	0.307	0.425	3810	8.2	127.7	75.6	44.9	223.7
15/10/2011	-26.3	0.293	0.423	4114	8.8	101.6	63.9	45.7	237.6
29/10/2011	-26.2	0.283	0.401	3679	8.1	105.2	67.4	44.3	239.3
12/11/2011	-26.7	0.266	0.426	5123	7.8	80.5	65.7	45.8	238.5
26/11/2011	-27.5	0.271	0.364	2958	7.6	91.9	63.0	43.9	242.0
10/12/2011	-28.0	0.288	0.375	2704	7.5	96.0	66.6	44.9	245.9
24/12/2011	-28.7	0.333	0.394	1934	6.7	94.3	75.4	52.9	233.1
14/01/2012	-29.9	0.386	0.430	1327	7.3	88.8	87.9	63.2	225.0
28/01/2012	-31.2	0.434	0.465	997	6.9	80.2	104.9	75.1	234.8
11/02/2012	-30.6	0.478	0.511	1088	6.5	79.4	119.3	85.4	231.7
24/02/2012	-29.5	0.523	0.533	451	6.6	128.2	135.1	92.7	218.5
10/03/2012	-29.1	0.579	0.590	481	6.3	137.5	146.5	103.2	212.1
31/03/2012	-29.5	0.663	0.695	1116	6.1	159.3	180.9	119.7	181.0

Supplementary Table 3 : Full dataset on physico-chemical and biogeochemical data collected in various tributaries of the Oubangui during 3 field campaings between 2010 and 2012.

Date	River / Site	Latitude (decimal degrees)	Longitude (decimal degrees)	T (°C)	$\%O_2$	Specific conductivity ($\mu S\ cm^{-1}$)	pH (NBS scale)	TSM ($mg\ L^{-1}$)	δ^{13}C-DIC (‰)	POC ($mg\ L^{-1}$)	PN ($mg\ L^{-1}$)	POC/PN (weight)	%POC	δ^{13}C-POC (‰)
21/03/2010	Mbali River	4.91439	18.00844	24.4	98.5	31.7	6.73	2.7	-11.1	0.277	0.034	8.1	12.3	-29.4
21/03/2010	Mbali River	4.66550	18.22128	26.7	88.4	52.8	7.39	3.1	-10.4	0.372	0.032	11.8	8.5	-27.5
21/03/2010	Mpoko River	4.32442	18.51167	29.1	78.2	170.2	7.59	77.0	-10.5	1.689	0.232	7.3	13.8	-22.8
22/03/2010	Lobaye, ferry point	4.05069	17.34492	26.4	94.6	13.0	6.45	15.0	-15.3	1.092	0.106	10.3	9.7	-28.1
23/03/2010	Lobaye, bridge	4.17358	17.22372	25.5	90.9	12.6	6.41	17.2	-16.2	1.427	0.121	11.8	8.5	-27.8
21/03/2011	Lobaye	4.07166	17.30829	25.5	98.7	11.9	6.90	14.4	-14.7	1.334	0.110	12.1	9.3	-28.8
21/03/2011	Lobaye	4.10503	17.29411	25.8	99.4	11.9	6.94	12.6	-13.9	1.158	0.099	11.7	9.2	-29.0
22/03/2011	Lobaye, after confluence with Mbaéré	3.75407	17.52856	26.2	91.7	11.3	6.63	10.4	-15.9	0.997	0.086	11.6	9.5	-29.3
22/03/2011	Lobaye	3.79562	17.49983	26.8	97	16.3	6.74	16.4	-13.8	1.426	0.136	10.5	8.7	-29.0
22/03/2011	Lobaye	3.87487	17.47599	26.6	99.5	13.1	6.98	12.8	-14.2	1.290	0.119	10.9	10.1	-29.0
20/11/2012	Lobaye	4.07166	17.30829	24.7	92	16.2	6.68	8.8	-18.0	1.057	0.075	14.1	12.1	-29.0
21/11/2012	Lobaye	3.92850	17.43455	25.1	92.1	18.3	6.84	6.6	-16.0	0.990	0.110	9.0	15.1	-29.3
21/11/2012	Lobaye	3.87355	17.46859	25.2	92.6	18.5	6.75	6.9	-18.1	1.124	0.241	4.7	16.2	-28.8
22/11/2012	Lobaye	3.79557	17.49878	25.5	91.8	21.3	6.79	12.4	-16.3	1.015	0.101	10.0	8.2	-29.1
22/11/2012	Lobaye, dowstream of confluence with Mbaéré	3.75726	17.53485	25.3	69.3	13.2	6.01	5.2	-20.7	0.648	0.062	10.5	12.4	-29.4
23/03/2010	Mbaére, bridge	3.94450	17.02500	24.5	63.2	8.2	5.56	5.5	-23.6	0.627	0.054	11.6	8.6	-29.3
20/03/2011	Mbaéré	3.90394	17.11073	25.5	64.4	7.6	6.26	5.6	-21.2	1.132	0.102	11.0	20.2	-29.7
20/03/2011	Mbaéré	3.89716	17.15729	25.3	79.4	7.9	6.27	8.6	-21.3	1.494	0.117	12.7	17.4	-30.0
23/03/2011	Mbaéré	3.80638	17.32200	25.7	80	8.4	5.71	6.4	-22.6	0.914	0.074	12.3	14.3	-30.5
23/03/2011	Mbaéré	3.84314	17.26092	25.6	79	8.1	5.70	6.6	-22.8	1.354	0.099	13.7	20.5	-30.2
23/11/2012	Mbaéré	3.89735	17.15737	24.7	51	8.1	5.30	1.2	-28.1	0.432	0.029	14.8	36.0	-29.8
22/03/2011	Mbaéré, after confluence with Bodingué	3.75467	17.51074	25.6	83	7.8	5.98	3.9	-22.1	0.888	0.071	12.5	23.0	-30.5
23/03/2011	Mbaéré, after confluence with Bodingué	3.75558	17.38182	25.7	80.5	8.7	5.62	5.6	-23.2	0.921	0.074	12.5	16.4	-30.7
22/11/2012	Mbaéré, after confluence with Bodingué	3.75453	17.51075	24.2	48.1	9.7	4.88	1.1	-26.5	0.348	0.024	14.4	30.5	-30.1
20/03/2011	Imbalataka (tributary of Mbaéré)	3.90408	17.11038	23.3	66.1	11.7	5.75	3.5	-22.9	0.903	0.079	11.4	26.1	-29.1
20/03/2011	Kélé (tributary of Mbaéré)	3.90082	17.15848	23	84.8	15.2	5.02	4.4	-24.1	1.821	0.137	13.3	41.4	-30.5
23/11/2012	Kélé (tributary of Mbaéré)	3.90075	17.15847	25.2	91.2	12.2	4.94	0.7	-22.5	0.408	0.038	10.7	55.1	-30.7
23/03/2011	Bodingué	3.75596	17.37455	25.4	76.8	8.8	5.31	2.1	-24.5	0.561	0.041	13.6	26.7	-31.2
21/03/2011	Mamboussou (right bank tributary of Lobaye)	4.08135	17.30740	22.8	90	36.6	6.86	38.3	-15.7	3.221	0.307	10.5	8.4	-29.2
20/11/2012	Mamboussou (right bank tributary of Lobaye)	4.08147	17.30735	22.4	87.5	52.6	7.13	28.2	-13.2	3.315	0.259	12.8	11.8	-29.1
21/03/2011	Ibéléké (right bank tributary of Lobaye)	4.02745	17.32564	24.8	85		6.50	10.4	-18.9	1.858	0.192	9.7	17.9	-30.0
24/11/2012	Ibéléké (right bank tributary of Lobaye)	4.02745	17.32564	23.3	93.5	20.0	6.26	14.1	-16.4	2.176	0.205	10.6	15.4	-30.2
21/03/2011	Lubé (left bank tributary of Lobaye)	4.06681	17.32090	23	90.6	97.1	7.25	44.4	-12.6	2.131	0.226	9.4	4.8	-25.8
20/11/2012	Unnamed left bank tributary of the Lobaye	4.06685	17.32090	23.5	87.2	99.5	7.42	35.9	-11.7	1.350	0.120	11.2	3.8	-25.8
21/11/2012	Ngilingala (left bank tributary of the Lobaye)	4.00858	17.38897	22.8	90.8	95.1	7.50	34.2	-13.4	1.275	0.118	10.8	3.7	-26.3
21/11/2012	Unnamed left bank tributary of Lobaye	3.96712	17.41333	23.6	88.4	87.7	7.09	9.4	-14.1	0.746	0.052	14.3	8.0	-29.3
21/11/2012	Loamé (left bank tributary of Lobaye)	3.84159	17.48700	25.1	90.3	67.7	7.27	36.2	-12.8	1.424	0.231	6.2	3.9	-27.5

Supplementary Table 3 (continued)

Date	River / Site	DOC (mg L-1)	δ^{13}C-DOC (‰)	TA (mmol L^{-1})	DIC (mmol L^{-1})	pCO_2 (ppm)	N_2O (nmol L^{-1})	CH_4 (nmol L^{-1})	Ca (µM)	Mg (µM)	Si (µM)
21/03/2010	Mbali River	2.2		0.275	0.390	3350	6.4	1652	49.8	36.8	212.5
21/03/2010	Mbali River	2.1		0.538	0.585	1476	7.3	452			
21/03/2010	Mpoko River	3.3		1.791	1.886	3253	9.3	779	469.2	311.3	271.8
22/03/2010	Lobaye, ferry point	2.5		0.131	0.234	3160	7.3	422	26.6	15.7	211.7
23/03/2010	Lobaye, bridge	4.4		0.119	0.222	3060	7.3	324			
21/03/2011	Lobaye	1.93	-28.2	0.118	0.151	981	8.3	358	25.1	15.0	203.9
21/03/2011	Lobaye	2.06	-28.6	0.113	0.142	870	8.4	252	24.9	15.0	210.3
22/03/2011	Lobaye, after confluence with Mbaéré	1.90	-29.0	0.119	0.181	1881	9.8	315	27.8	17.4	200.7
22/03/2011	Lobaye	1.74	-27.3	0.148	0.207	1822	9.0	321	36.4	22.7	211.4
22/03/2011	Lobaye	1.93	-28.7	0.126	0.155	887	8.8	291	27.2	17.2	212.8
20/11/2012	Lobaye	3.10	-28.4	0.161	0.236	2202	7.3	256	39.0	20.2	223.7
21/11/2012	Lobaye	3.25	-28.1	0.189	0.250	1796	7.5	451	42.4	23.3	230.8
21/11/2012	Lobaye	3.23	-28.1	0.184	0.258	2185	7.4	388	44.3	23.3	237.7
22/11/2012	Lobaye	2.99	-28.4	0.208	0.283	2237	7.8	686	54.1	29.4	233.4
22/11/2012	Lobaye, dowstream of confluence with Mbaéré	5.04	-29.7	0.107	0.343	6990	7.2	457	37.0	16.6	217.0
23/03/2010	Mbaére, bridge	4.4		0.059	0.447	11180	8.7	730	14.0	8.3	180.3
20/03/2011	Mbaéré	1.50	-29.7	0.060	0.135	2203			14.2	7.9	179.6
20/03/2011	Mbaéré	1.66	-29.9	0.058	0.130	2104	10.0	711	14.5	7.9	174.3
23/03/2011	Mbaéré	2.95	-29.7	0.059	0.325	7911	10.0	515	14.3	8.6	182.4
23/03/2011	Mbaéré	2.60	-29.9	0.055	0.313	7631	10.0	561	14.1	8.3	183.1
23/11/2012	Mbaéré	5.71	-30.3	0.037	0.515	13813	7.1	516	20.4	7.1	171.7
22/03/2011	Mbaéré, after confluence with Bodingué	2.42	-30.0	0.061	0.207	4318	10.9	365	13.7	8.3	209.4
23/03/2011	Mbaéré, after confluence with Bodingué	3.46	-29.9	0.050	0.331	8347	10.2	418	15.2	8.7	179.6
22/11/2012	Mbaéré, after confluence with Bodingué	7.10	-30.4	0.026	1.201	33500	7.8	451	18.6	6.1	168.0
20/03/2011	Imbalataka (tributary of Mbaéré)	1.27	-29.9	0.034	0.180	4045	13.0	374	18.7	12.4	167.3
20/03/2011	Kélé (tributary of Mbaéré)	4.45	-30.2	0.029	0.875	23255	26.7	254	14.5	9.4	136.6
23/11/2012	Kélé (tributary of Mbaéré)	0.76	-30.6	0.009	0.556	15849	26.2	107	23.8	7.3	158.8
23/03/2011	Bodingué	4.30	-30.1	0.038	0.517	14070	11.5	442	13.4	8.7	175.4
21/03/2011	Mamboussou (right bank tributary of Lobaye)	12.23	-29.2	0.256	0.337	2237	10.8	1213	69.3	47.4	341.8
20/11/2012	Mamboussou (right bank tributary of Lobaye)	6.02	-29.5	0.512	0.600	2432	8.2	1275	108.6	79.8	407.9
21/03/2011	Ibéléké (right bank tributary of Lobaye)	3.24	-29.7	0.111	0.191	2334	9.5	2587	22.1	17.1	209.1
24/11/2012	Ibéléké (right bank tributary of Lobaye)	3.16	-30.1	0.164	0.374	5897	8.4	2168	41.2	24.0	224.3
21/03/2011	Lubé (left bank tributary of Lobaye)	5.50	-27.1	0.903	1.020	3271	10.6	821	190.9	157.6	490.1
20/11/2012	Unnamed left bank tributary of the Lobaye	3.43	-27.0	0.991	1.075	2412	8.3	917	181.9	167.7	545.2
21/11/2012	Ngilingala (left bank tributary of the Lobaye)	3.74	-28.1	0.948	1.016	1927	8.5	1045	175.0	191.8	560.9
21/11/2012	Unnamed left bank tributary of Lobaye	3.11	-28.3	0.714	0.846	3768	9.4	2911	149.1	141.6	436.1
21/11/2012	Loamé (left bank tributary of Lobaye)	2.75	-28.3	0.664	0.743	2363	8.5	726	166.0	114.2	303.8

Supplementary Table 4: CDOM parameters of various tributaries of the Oubangui River during 2 field compaings in 2011 and 2012.

Date	River/Site	DOC	$a_{350}(m^{-1})$	$a_{250}:a_{365}$	$S_{275-295}$ (nm^{-1})	$S_{350-400}$ (nm^{-1})	S_R
21/03/2011	Lobaye	1.93	8.8	4.1	0.0126	0.0156	0.8072
21/03/2011	Lobaye	2.06	9.8	3.9	0.0125	0.0151	0.8302
22/03/2011	Lobaye. after confl with Mbaéré	1.90	10.0	3.9	0.0122	0.0150	0.8131
22/03/2011	Lobaye	1.74	9.5	3.9	0.0119	0.0148	0.8063
22/03/2011	Lobaye	1.93	11.8	3.7	0.0118	0.0145	0.8171
20/11/2012	Lobaye	3.10	19.1	3.7	0.0114	0.0148	0.7675
21/11/2012	Lobaye	3.25	19.5	3.7	0.0111	0.0147	0.7551
21/11/2012	Lobaye	3.23	16.8	3.8	0.0119	0.0151	0.7857
22/11/2012	Lobaye	2.99	15.4	3.9	0.0121	0.0152	0.7934
22/11/2012	Lobaye. dowstream of confluence with Mbaéré	5.04	27.9	3.6	0.0114	0.0145	0.7807
20/03/2011	Mbaéré	1.50	8.4	4.1	0.0124	0.0144	0.8630
20/03/2011	Mbaéré	1.66	9.7	4.0	0.0123	0.0134	0.9167
23/03/2011	Mbaéré	2.95	13.5	4.1	0.0125	0.0146	0.8563
23/03/2011	Mbaéré	2.60	13.4	3.9	0.0120	0.0144	0.8370
23/11/2012	Mbaéré	5.71	29.0	3.8	0.0114	0.0147	0.7808
22/03/2011	Mbaéré. after confl with Bodingué	2.42	10.5	4.3	0.0131	0.0152	0.8605
23/03/2011	Mbaéré. after confl with Bodingué	3.46	15.7	4.0	0.0126	0.0144	0.8732
22/11/2012	Mbaéré. after confl with Bodingué	7.10	35.0	3.7	0.0117	0.0146	0.7987
20/03/2011	Imbalataka (tributary) of Mbaéré	1.27	6.9	3.7	0.0117	0.0125	0.9343
20/03/2011	Kélé (tributary of Mbaéré)	4.45	14.7	4.3	0.0129	0.0143	0.8967
23/11/2012	Kélé (tributary of Mbaéré)	0.76	5.3	3.7	0.0115	0.0127	0.9016
23/03/2011	Bodingué	4.30	17.7	4.1	0.0125	0.0147	0.8564
20/11/2012	Mamboussou (right bank tributary of Lobaye)	6.02	25.7	4.0	0.0119	0.0154	0.7742
21/03/2011	Ibélélé (right bank tributary of Lobaye)	3.24	14.2	4.0	0.0123	0.0154	0.7973
24/11/2012	Ibélélé (right bank tributary of Lobaye)	3.16	16.0	4.0	0.0118	0.0154	0.7644
21/03/2011	Lubé (left bank tributary of Lobaye)	5.50	17.4	4.2	0.0124	0.0163	0.7576
20/11/2012	Unnamed left bank tributary of Lobaye	3.43	16.4	4.0	0.0118	0.0163	0.7235
21/11/2012	Ngilingala (left bank tributary of Lobaye)	3.74	16.2	4.1	0.0120	0.0164	0.7356
21/11/2012	Unnamed left bank tributary of Lobaye	3.11	15.2	4.0	0.0117	0.0170	0.6868
21/11/2012	Loamé (left bank tributary of Lobaye)	2.75	15.0	3.7	0.0115	0.0158	0.7285

Supplementary Table 5: Temporal variations of CDOM parameters in the Oubangui mainstream.

Date	a_{350} (m^{-1})	a_{250}:a_{365}	$S_{275-295}$ (nm^{-1})	$S_{350-400}$ (nm^{-1})	S_R
17/03/2011	5.6	5.0	0.0161	0.0137	1.1745
14/04/2011	5.2	5.0	0.0164	0.0128	1.2741
28/04/2011	5.3	5.2	0.0170	0.0130	1.2990
14/05/2011	4.8	5.4	0.0168	0.0127	1.3234
28/05/2011	5.9	5.5	0.0171	0.0136	1.2549
16/06/2011	10.0	5.1	0.0159	0.0145	1.0984
28/06/2011	12.9	4.7	0.0151	0.0155	0.9742
13/07/2011	16.9	4.4	0.0141	0.0154	0.9101
30/07/2011	18.0	4.2	0.0137	0.0150	0.9108
13/08/2011	20.1	4.1	0.0130	0.0149	0.8691
30/08/2011	23.6	4.3	0.0130	0.0159	0.8137
10/09/2011	24.0	4.3	0.0131	0.0159	0.8195
25/09/2011	22.4	4.2	0.0129	0.0158	0.8206
15/10/2011	22.5	4.3	0.0131	0.0160	0.8169
29/10/2011	23.2	4.2	0.0128	0.0159	0.8035
12/11/2011	25.1	4.2	0.0127	0.0157	0.8132
26/11/2011	22.8	4.2	0.0126	0.0157	0.7979
10/12/2011	22.0	4.1	0.0125	0.0156	0.7995
24/12/2011	19.2	3.7	0.0118	0.0147	0.8050
11/02/2012	3.8	4.6	0.0126	0.0122	1.0273
24/02/2012	6.9	4.7	0.0157	0.0144	1.0919
10/03/2012	7.3	4.6	0.0168	0.0135	1.2468
31/03/2012	5.1	5.2	0.0168	0.0139	1.2109